

Random lasing from Anderson attractors

Guillaume Rollin,¹ José Lages,¹ and Dima L. Shepelyansky²

¹*Institut UTINAM, UMR 6213, CNRS, Université Bourgogne Franche-Comté Besançon, France*

²*Laboratoire de Physique Théorique, Université de Toulouse, CNRS, UPS, 31062 Toulouse, France*

(Dated: January 11, 2022)

We introduce and study a two-dimensional dissipative nonlinear Anderson pumping model which is characterized by localized or delocalized eigenmodes in a linear regime and in addition includes nonlinearity, dissipation and pumping. We find that above a certain pumping threshold the model has narrow spectral lasing lines generated by isolated clusters of Anderson attractors. With the increase of the pumping, the lasing spectrum is broadened even if narrow lasing peaks are still well present in the localized phase of linear modes. In the metallic phase, the presence of narrow spectral peaks is significantly suppressed. We argue that the model captures main features observed for random lasers.

PACS numbers:

I. INTRODUCTION

The theory of random lasing in a disordered active media was introduced by V.S. Letokhov in 1967-1968 [1]. At present, various types of random lasers operating in different gain and scattering media, including powder and fibers, have been experimentally realized as reviewed in [2–5]. The active interest to random lasers is stimulated not only by their technological applications but also by a variety of inter-disciplinary links to other research fields, such as the theory of disordered and mesoscopic systems [6], Anderson localization and transport [7, 8], nonlinear waves in disordered media [9, 10], chaotic dynamics and strange attractors [11, 12], synchronization [13], material science, spectroscopy and laser physics (see e.g. [14]).

Due to such an interdisciplinary nature and complexity of random lasing systems, deep theoretical studies are required with applications of advanced analytical and numerical tools and methods. Various numerical studies have been reported with the main objective to explain specific features of random lasing observed in experiments (see e.g. [15, 16]). However, an interplay on nonlinearity, disorder, dissipation and pumping results in a rather complex dynamics which the properties are rather difficult to capture and investigate in studies of specific modeling of an experimental setup. Due to these reasons, we introduce here a simplified Dissipative Nonlinear Anderson Pumping (DINAP) model which in various limiting regimes describes such generic phenomena as Anderson localization, transport in disordered media, nonlinear waves, dissipation, pumping, synchronization, and chaotic dissipative dynamics. We show that a lasing in such a model captures the main features of random lasers.

II. MODEL DESCRIPTION

The DINAP model is described by the time evolution equations

$$\begin{aligned} i\dot{A}_{x,y} = & E_{x,y}A_{x,y} + \beta |A_{x,y}|^2 A_{x,y} + (1 - i\eta)(-A_{x,y+1} \\ & + 4A_{x,y} - A_{x,y-1} - A_{x+1,y} - A_{x-1,y}) \\ & + i(\alpha - \sigma |A_{x,y}|^2) A_{x,y}. \end{aligned} \quad (1)$$

Here, $A_{x,y}$ is the radiation field amplitude on the site (x, y) of a $N \times N$ square lattice with periodic boundary conditions, $E_{x,y}$ are on site unperturbed energies randomly distributed in the $[-W/2, W/2]$ interval. For $\beta = \eta = \alpha = \sigma = 0$, the model is reduced to the two-dimensional Anderson model (see e.g. [8]) with a unit hopping amplitude on nearby sites. In absence of disorder, i.e. at $W = 0$, the spectrum of linear waves on a lattice of size $N \times N$ has the form $\lambda_{q_x, q_y} = 4 - 2 \cos(2\pi q_x/N) - 2 \cos(2\pi q_y/N)$, where q_x and q_y are wave numbers of ballistic waves. In presence of disorder, i.e. $W > 0$, all the eigenstates are exponentially localized but the localization length increases exponentially with a decrease of the disorder strength W [6, 8]. For a lattice of finite size $N \sim 100$, the eigenstates are well localized at $W = 6 - 8$ [17].

For finite β and $\eta = \alpha = \sigma = 0$, the DINAP model is reduced to the 2D Discrete Anderson Nonlinear Schrödinger equation (DANSE) model which was actively studied for the investigation of effects of weak nonlinearity on the Anderson localization (see e.g. [18–20]). It was shown that a moderate nonlinearity leads to a destruction of the localization and a subdiffusive spreading of the field over the lattice.

The DINAP model has several new features compared to the unitary DANSE model. Indeed, the parameter α describes lasing instability of the nonlinear media which is balanced by the linear damping η -term and the more significant nonlinear damping σ -term. Due to that, the DINAP model captures various nontrivial features of the nonlinear lasing in dissipative media with disorder. Due to nonlinearity and disorder, it is natural to expect that

the dynamics will be characterized by the presence of chaotic attractors which are typical for nonlinear dissipative systems [11, 12].

We note that a similar model in 1D was studied in [21]. A number of interesting results have been reported there. In our studies, we analyze a more realistic 2D case and concentrate the investigations on the lasing spectrum produced by the nonlinear media of DINAP model.

The numerical integration of the coupled equations (1) is done in the frame of the Trotter decomposition used in [18, 19]. This integration scheme is symplectic (at $\eta = \alpha = \sigma = 0$) and allows to perform accurate numerical simulations on large time scales. The physical arguments which explain the accuracy and the advantages of such integration are described in [22].

In the numerical simulations, we usually use the integration time step, $\Delta = 0.1$, checking that the variation of this step by several times is not affecting the obtained results. The main part of the results is presented for the lattice size $N \times N = 128 \times 128$. Such a size is significantly larger than the localization length of linear eigenstates with a typical disorder strength $W = 8$.

At the initial time $t = 0$, a field $A_{x,y}$ is taken as random with typical amplitudes $|A_{x,y}|^2 \approx 7 \times 10^{-11}$ with a standard deviation being approximately 4×10^{-11} . For a fixed random configuration of the energies $E_{x,y}$, the initial field amplitudes do not influence the field amplitudes at large times $t \sim 10^5$ (steady-state) since the field time evolution converges to fixed Anderson attractors distributed on the lattice. This Anderson attractor steady state, averaged over a moderate time interval $\Delta t \sim 10^3$, is independent of the above described initial random field realization $A_{x,y}$.

The obtained numerical results are described in the next section.

III. RESULTS

In Fig. 1, we show the dependence of the space averaged steady-state field power $P = \langle |A_{x,y}|^2 \rangle$ on the rescaled active media parameter α/η . The field growth is generated by an effect of active media described by the parameter α growth. The dissipative effects are produced by the η -term. The field growth is limited by the nonlinear dissipative σ -term. Thus, at small values of the ratio α/η , the generated field remains small so that $P \ll 1$ for $\alpha/\eta < 0.7$. In contrast, above the threshold value $\alpha/\eta \approx 0.7$, the field power is growing significantly that corresponds to the random lasing regime. We note that a similar behavior has been described for the 1D model [21].

Typical distributions of the lasing power $w(x,y) = |A_{x,y}|^2$ on the 2D lattice are shown in Fig. 2 for different values of the activation strength α . The results show a significant increase of the number of lasing attractors with the growth of the α -parameter (see Fig. 2 a,b,c panels). The Anderson attractor is the steady state of the

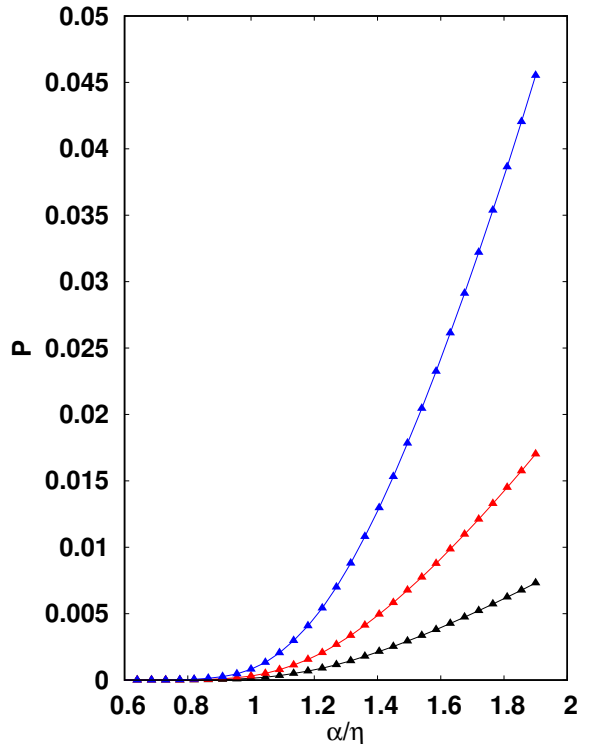


FIG. 1: Dependence of the space averaged steady-state field power $P = \langle |A_{x,y}|^2 \rangle$ on the active media parameter α/η . Here, the parameters are $W = 8$, $\beta = \sigma = 1$. For $\eta = 0.1$, the steady-state is obtained at $t_e = 10^4$ with an averaging over time interval $\Delta t = 10^3$. The lattice size is 128×128 . The values of the linear damping are $\eta = 0.2$ (blue points), $\eta = 0.1$ (red points), and $\eta = 0.05$ (black points).

system since once established, e.g. at $t_e = 10^4$ (see panel a), it continues for longer times, e.g. at $t = 10^5$ (the lasing power distributions are the same in a and d panels). The results are shown for a typical initial field distribution with random amplitudes $A_{x,y}$ described in the previous section; we numerically check that any choice of other random configurations $A_{x,y}$ does not change the average lasing distribution.

Using the fast Fourier transform, we determine the spectrum of the random lasing defined as $Z(\omega) = \langle |\int dt A_{x,y}(t) \exp(-i\omega t)|^2 \rangle$ where the $\langle \rangle$ -brackets denote the averaging over the whole lattice space. We also compute the integral of the spectral power of the random lasing $Z_{tot} = \int d\omega Z(\omega)$. The spectrum $Z(\omega)$ of the random lasing is shown in Fig. 3 together with the lasing power distribution $w(x,y)$ over the lattice. For small activation strength $\alpha = 0.09$, the lasing spectrum is composed of well separated strong frequency peaks (Fig. 3d). The space distribution (Fig. 3a) indicates that these frequency peaks are generated by well separated lattice cells (clusters). We call this regime a regime of random lasing clusters. With the increase of the pumping strength $\alpha = 0.31$, the lasing spectrum becomes rather broad even if there are still a couple of dominant strong frequency

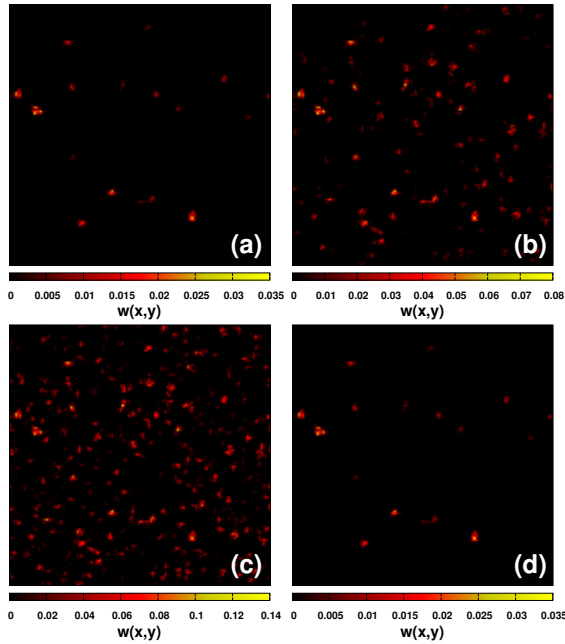


FIG. 2: Anderson attractor in the DINAP model for a 2D lattice with a linear size $N = 128$, a disorder strength $W = 8$, $\beta = \sigma = 1$, and $\eta = 0.1$. The different panels show the lasing power distribution $w(x, y) = |A_{x,y}|$ for the pumping strength $\alpha = 0.09$ (a,d), $\alpha = 0.11$ (b), and $\alpha = 0.13$ (c). The lasing power distributions are shown after an evolution time $t_e = 10^4$ (a,b,c) and $t_e = 10^5$ (d). The panel (d) shows the attractor stability for long evolution times. The color bars give the values of $w(x, y)$. The $w(x, y)$ distributions are averaged over a time interval $\delta t = 10^3$.

peaks emerging from a quasi-continuum spectral component (Fig. 3e). Over the lattice, see Fig. 3b, there are more and more lasing sites as α increases. At stronger pumping strength, e.g. $\alpha = 0.91$, the lasing spectrum becomes almost continuous (Fig. 3f), and over the lattice, almost all the sites are lasing (Fig. 3c).

To demonstrate that indeed spectral peaks are generated by specific isolated clusters, we select three groups of sites for the small activation strength $\alpha = 0.09$ delimited by the red, green, and blue color squares in Fig. 3a. In Fig. 4, we superimpose the lasing spectrum of each of the 3 selected clusters onto the lasing spectrum obtained for the whole lattice. Fig. 4 results clearly show that these 3 selected clusters generate well isolated spectral peaks of lasing.

Of course, for another random realization of the on-site energies $E_{x,y}$, and for small, moderate and strong activation strengths $\alpha = 0.09, 0.31, 0.91$, the location of clusters are different but the global picture of lasing is similar to those shown in Figs. 2 and 3 which describe a generic situation.

In the above presented figures, we considered the case when the linear system (ie, the linear modes of the corresponding Anderson model) has well localized eigenstates with a localization support being significantly smaller

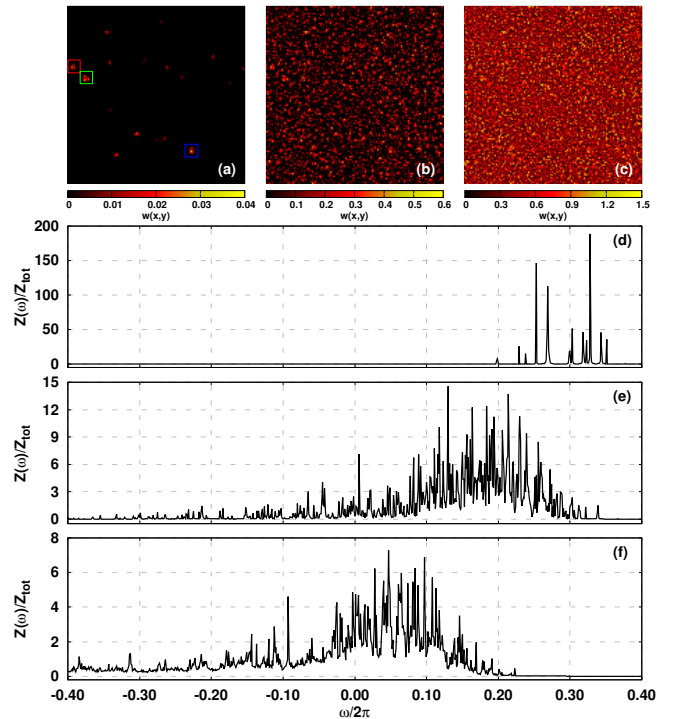


FIG. 3: Spectrum $Z(\omega)$ of random lasing in the DINAP model for a 2D lattice with a linear size $N = 128$, a disorder strength $W = 8$, $\beta = \sigma = 1$, and $\eta = 0.1$ (same parameters as in Fig. 2). The pumping strength is $\alpha = 0.09$ (a,d), 0.31 (b,e), and 0.91 (c,f). The (a,b,c) panels show the lasing power distributions $w(x, y)$ and the (d,e,f) panels show the spectrum $Z(\omega)$ of the random lasing. The integral of the spectral lasing power is $Z_{tot} \simeq 8.7 \times 10^{-8}$ (a,d), 6.0×10^{-5} (b,e), and 4.5×10^{-4} (c,f). Initial conditions and random realizations are the same as in Fig. 2(a,d).

than the linear system size N (see the typical eigenstate characteristics for $W = 8$ at [17]). This regime is characterized by narrow peaks of lasing spectrum generated by isolated localized clusters. It is also interesting to consider the opposite case when linear modes have a support being comparable to the linear system size thus corresponding to the metallic regime. For $W = 3$, we have approximately such a regime according to the results presented in [17]. The power distribution $w(x, y)$ over the lattice and the lasing spectrum $Z(\omega)$ for such a case are shown in Fig. 5. In this metallic regime, even for a small activation strength $\alpha = 0.09$, we have a broad spatial power distribution of lasing; the lasing spectrum is quasi-continuous. For strong activation strength $\alpha = 0.91$, almost all the lattice sites are lasing. The lasing spectrum has a structure being similar to the one for small $\alpha = 0.09$ but with a larger number of spectral peaks. The important feature of the metallic regime at $W = 3$ is that all spectral peaks visible in the localized regime at $W = 8$ are replaced by a quasi-continuous broad distribution. Thus, the localized regime is better adapted to a narrow spectral line of lasing.

The integrated lasing power, taking the same pump-

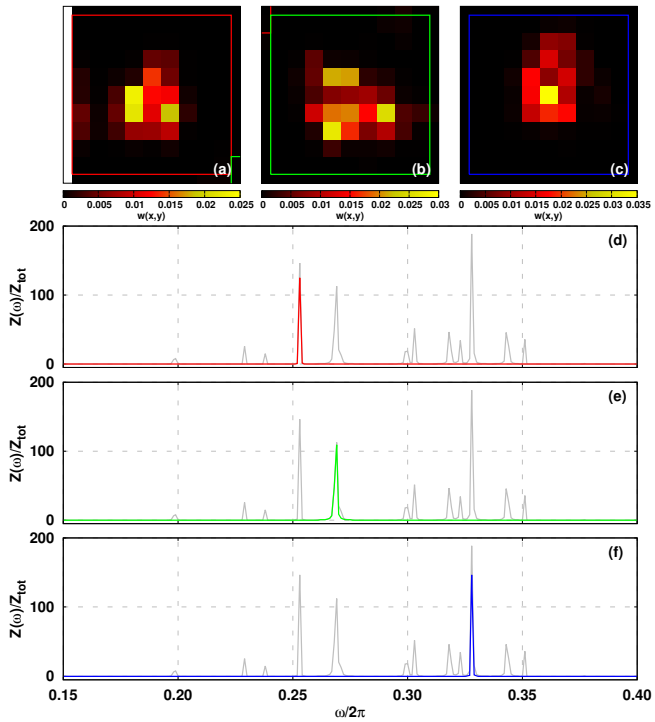


FIG. 4: The lasing clusters present in the red, green and blue squares in the Fig. 3a are shown in the a, b and c panels, respectively. The frequencies activated by these clusters are shown by the red, green and blue curves in the d, e and f panels, respectively. The spectrum $Z(\omega)$ of the whole attractor (Fig. 3d) is drawn in the background of the d, e and f panels. Here, the random lasing spectrum $Z(\omega)$ is normalized by the integral $Z_{tot} \simeq 8.7 \times 10^{-8}$.

ing and dissipation parameters, is globally higher for the metallic phase regime (see e.g. Fig. 5cf with $W = 3$, $Z_{tot} \simeq 7.5 \times 10^{-4}$) than for the localized phase regime (see e.g. Fig. 3cf with $W = 8$, $Z_{tot} = 4.5 \times 10^{-4}$). We attribute this to the fact that more sites contribute to the lasing in the metallic phase due to delocalized eigenstates of the linear Anderson model.

IV. DISCUSSION

We introduced a mathematical 2D DINAP model to describe specific features of the random lasers: lasing above a certain threshold, pronounced spectral lasing peaks, lasing clusters. Our numerical analysis shows that these features are well described by the DINAP model. The important element of the model is that in the linear regime without nonlinearity and dissipation it is reduced to the 2D Anderson model with localized modes at strong disorder and delocalized ones at weak disorder when the finite system size becomes comparable with 2D localization length (in the infinite system). In the localized phase, above the critical pumping strength α , the spectrum of lasing is composed of narrow spectral lines.

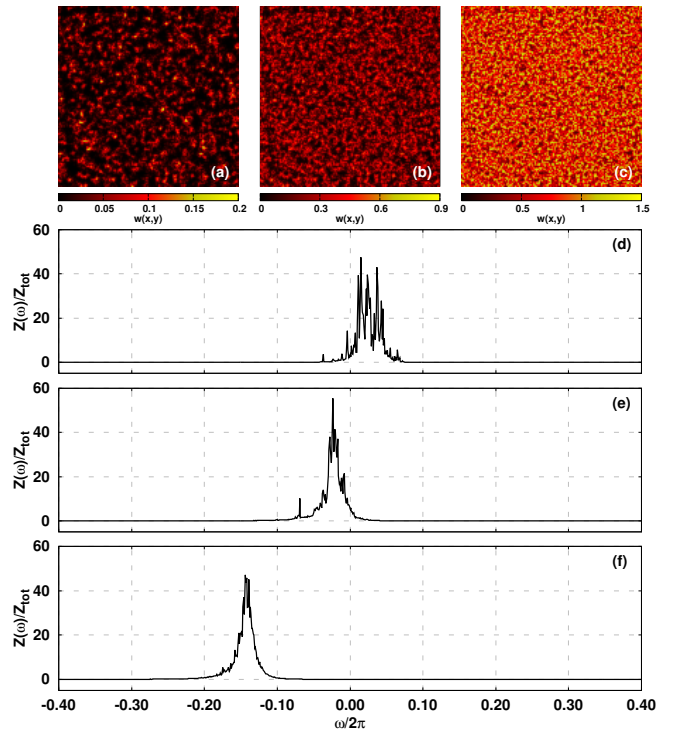


FIG. 5: Same as in Fig. 3 but for a disorder strength $W = 3$. Here, $Z_{tot} \simeq 2.41 \times 10^{-5}$ for $\alpha = 0.09$ (a,d), 1.9×10^{-4} for $\alpha = 0.31$ (b,e), and 7.5×10^{-4} for $\alpha = 0.91$ (c,f).

These lines emanate from localized isolated clusters located in a media where a nonlinear dissipative dynamics leads to isolated Anderson attractors. With the increase of the pumping strength, the lasing peaks are still present but a global envelope appears corresponding to lasing from a large number of connected or disconnected clusters. Globally, an increase of the pumping strength leads to a broader lasing spectrum. We find that such an effect is rather natural since with the increase of the pumping, the nonlinear frequency corrections become higher. In the metallic regime, the peaks are significantly less visible even if only slightly above the threshold pumping and at higher strength of pumping, the lasing spectrum gets a form of a smooth envelope. We attribute this feature to a delocalized structure of linear modes where nonlinear frequency corrections at high pumping get contribution from many lattice sites on which are located the delocalized linear modes.

In the localized phase, our results show that a percolation transition takes place from a localized lasing clusters regime to a delocalized regime of lasing from many lattice sites when the strength of the pumping significantly increases above the threshold value. There is a number of interesting questions about such a percolation: What is the critical percolation threshold? How it depends on the system parameters? Is there a global synchronization of lasing, like the Kuramoto transition [13]? Is there a superradiance in such a synchronized phase? We think that the answers to these questions can be obtained in

the further investigations of the DINAP model.

INA) in the frame of the *Programme des Investissements d'Avenir, France*.

Acknowledgments

This research has been partially supported through the grant NANOX N° ANR-17-EURE-0009 (project MTD-

-
- [1] V.S. Letokhov, *Generation of light by a scattering medium with negative resonance absorption*, Sov. Phys.—JETP **26**, 835 (1968).
- [2] H. Cao, *Lasing in random media*, Waves in Random Media **13**(3), R1 (2003).
- [3] H. Cao, *Review on latest developments in random lasers with coherent feedback*, J. Phys. Math. Gen. **38**(49) 10497 (2005).
- [4] L. Sapienza, H. Thyrestrup, S. Stobbe, P.D. Garcia, S. Smolka and P. Lodahl, *Cavity quantum electrodynamics with Anderson-localized modes*, Science **327**, 1352 (2010).
- [5] S.K. Turitsyn, S.A. Babin, D.V. Churkin, I.D. Vatnik, M. Nikulin, and E.V. Podivilov, *Random distributed feedback fibre lasers*, Physica Reports **542**, 133 (2014).
- [6] E. Akkermans and G. Montambaux, *Mesoscopic physics of electrons and photons*, Cambridge Univ. Press, Cambridge (2007).
- [7] P.W. Anderson, *Absence of diffusion in certain random lattices*, Phys. Rev. **109**, 1492 (1958).
- [8] F. Evers, and A.D. Mirlin, *Anderson transitions*, Rev. Mod. Phys. **80**, 1355 (2008).
- [9] S.A. Gredeskul, and Y.S. Kivshar, *Propagation and scattering of nonlinear waves in disordered systems*, Physics reports **216**, 1 (1992).
- [10] S.E. Skipetrov, A. Minguzzi, B.A. van Tiggelen, and B. Shapiro, *Anderson localization of a Bose-Einstein condensate in a 3D random potential*, Phys. Rev. Lett. **100**, 165301 (2008).
- [11] A.J. Lichtenberg, and M. Lieberman, *Regular and chaotic Dynamics*, Springer, Berlin (1992).
- [12] E. Ott, *Chaos in dynamical systems*, Cambridge Univ. Press, UK (2002).
- [13] A. Pikovsky, M. Rosenblum, and J. Kurths, *Synchronization: a universal concept in nonlinear sciences*, Cambridge University Press, Cambridge UK (2001),
- [14] M.D. Levenson, and S.S. Kano, *Introduction to nonlinear laser spectroscopy*, Academic Press Inc., New York (1988).
- [15] H.E. Tureci, L. Ge, S. Rotter, and A.D. Stone, *Strong interactions in multimode random lasers*, Science **320**, 643 (2008).
- [16] P. Stano and P. Jacquod, *Suppression of interactions in multimode random lasers in the Anderson localized regime*, Nature Photon. **7**, 66 (2013).
- [17] J.Lages and D.L. Shepelyansky, *Phase of bi-particle localized states for the Cooper problem in two-dimensional disordered systems*, Phys. Rev. B **64**, 094502 (2001).
- [18] A.S. Pikovsky, and D.L. Shepelyansky, *Destruction of Anderson localization by a weak nonlinearity*, Phys. Rev. Lett. **100**, 094101 (2008).
- [19] I. Garcia-Mata, and D.L. Shepelyansky, *Delocalization induced by nonlinearity in systems with disorder*, Phys. Rev. E **79**, 026205 (2009).
- [20] T.V. Lapteva, M.I. Ivanchenko, and S. Flach, *Nonlinear lattice waves in heterogeneous media*, J. Phys. A: Math. Theor. **47**: 493001 (2014).
- [21] T.V. Lapyteva, A.A. Tikhomirov, O.I. Kanakov, and M.V. Ivanchenko, *Anderson attractors in active arrays*, Sci. Reports **5**, 13263 (2015).
- [22] L. Ermann and D.L. Shepelyansky, *Deconfinement of classical Yang-Mills color fields in a disorder potential*, CHAOS **31**, 093106 (2021).